IOPscience iopscience.iop.org

Home Search Collections Journals About Contact us My IOPscience

Influence of Si doping on optical properties of wurtzite GaN

This article has been downloaded from IOPscience. Please scroll down to see the full text article.

2001 J. Phys.: Condens. Matter 13 8891

(http://iopscience.iop.org/0953-8984/13/40/303)

View the table of contents for this issue, or go to the journal homepage for more

Download details:
IP Address: 171.66.16.226
The article was downloaded on 16/05/2010 at 14:55

Please note that terms and conditions apply.

INSTITUTE OF PHYSICS PUBLISHING JOURNAL OF PHYSICS: CONDENSED MATTER
J. Phys.: Condens. Matter **13** (2001) 8891–8899 PII: S0953-8984(01)24495-6

Influence of Si doping on optical properties of wurtzite GaN

A Ferreira da Silva[1], **C Moysés Araújo**[1], **Bo E Sernelius**[2], **C Persson**[3], **R Ahuja**[3] **and B Johansson**[3]

[1] Instituto de Física, Universidade Federal da Bahia, 40210-340 Salvador, Bahia, Brazil
[2] Solid State Division, Oak Ridge National Laboratory, Oak Ridge, TN 37831-6032, USA
[3] Department of Physics, Uppsala University, SE-75121 Uppsala, Sweden

Received 3 May 2001
Published 20 September 2001
Online at stacks.iop.org/JPhysCM/13/8891

Abstract
The band gap shift (BGS) of Si-doped wurtzite GaN for impurity concentrations spanning the insulating to the metallic regimes has been investigated at low temperature. The critical impurity concentration for the metal–non-metal transition is estimated from the generalized Drude approach for the resistivity to be about 1.0×10^{18} cm^{-3}. The calculations for the BGS were carried out within a framework of the random phase approximation, taking into account the electron–electron, electron–optical phonon, and electron–ion interactions. In the wake of very recent photoluminescence measurements, we have shown and discussed the possible transitions involved in the experimental results.

1. Introduction

GaN-based wide band gap semiconductors have drawn much current intensive research, mostly because of their potential applications for optical devices such as blue-green light emitting diodes and high-temperature electronics [1–14]. Despite its technological importance, there has so far been no reported detailed investigation of the band gap shift (BGS) of this material in the presence of high doping. The role of impurities is very important in fabricating devices. The efficiency of these devices is strongly affected by the incorporation of impurities. Experiments on doped semiconductors, above the impurity critical concentration N_c for the metal–non-metal (MNM) transition, reveal a BGS greater than 10% of the band gap of the pure material [14–16]. The value N_c is estimated here from the generalized Drude approach (GDA) for the resistivity.

At high doping levels the donor electrons are collected at the bottom of the conduction band. There are two quantities related to the band gap that are of interest. The energy distance between the Fermi level and the valence-band top, $E_{G,1}$, and the distance between the conduction and valence-band extrema, $E_{G,2}$. The latter energy is called the reduced band gap energy, which can be determined from optical emission measurements such as

 © 2001 IOP Publishing Ltd Printed in the UK

photoluminescence, whereas the former energy is called the optical band gap energy. The first is equal to the reduced band plus the band gap filling. The second is equal to the band gap in the absence of doping, $E_{G,0}$, plus the self-energy shifts of the states at the band extrema. In the wake of very recent photoluminescence spectroscopy which measured the BGS of wurtzite Si-doped GaN at low temperature, 2 K [14], we have compared the energies obtained experimentally with those calculated from three methods based on the random-phase approximation (RPA) [15–19] and discussed the possible transitions involved.

In a model expounded by Berggren and Sernelius [17] and simplified by Jain *et al* [18] and Lindefelt [19] the BGS has also been investigated.

2. Electrical resistivity and MNM transition

The generalized Drude approach was applied to polar semiconductors by Sernelius and Morling [20]. The results were based on the dynamical conductivity derived by Sernelius [21]. The static resistivity in a polar semiconductor is the same as for a non-polar semiconductor for which the expressions are simpler. Since here we are only interested in the static results we use the expressions for a non-polar semiconductor as a starting point.

For non-polar semiconductors the generalized Drude approach for the resistivity is reduced to [22]

$$\rho(\omega) = \frac{-\mathrm{i}m^*\omega}{ne^2} + \frac{\mathrm{i}2}{3\pi n\omega}\int_0^\infty q^2\left[\frac{1}{\varepsilon_T(q,\omega)} - \frac{1}{\varepsilon_T(q,0)}\right]\mathrm{d}q \tag{1}$$

where e is the electric charge, m^* is the effective mass and ε_T is the total dielectric function and n is the ionized impurity concentration. We have assumed a random distribution of Coulomb impurities. The total dielectric function is given by [21, 22]

$$\varepsilon_T(q,\omega) = \varepsilon + \alpha_1(q,\omega) + \mathrm{i}\alpha_2(q,\omega) \tag{2}$$

where ε is the dielectric constant of GaN, and α_1 and α_2 are the real and imaginary parts of the polarizabilities of doping carriers. These functions are temperature dependent. The imaginary part α_2 can be obtained analytically in the RPA [21, 22], The real part α_2 can be obtained from the imaginary part through the Kramers–Kroning dispersion relation.

We are interested in the static resistivity, which can now be written as [22]

$$\rho(0) = \frac{4\pi}{E_F}\int_0^\infty Q^2 \frac{[\partial\alpha_2(Q,W)/\partial W]|_{W=0}}{[\varepsilon + \alpha_1(Q,0)]^2}\,\mathrm{d}Q. \tag{3}$$

This can be reduced to [22]

$$\rho(0) = \frac{2(m^*e)^2}{3\pi n\hbar^3}\int_0^\infty \frac{\{1 - \tanh[0.5B(Q^2 - M)]\}}{Q[\varepsilon + \alpha_1(Q,0)]^2}\,\mathrm{d}Q \tag{4}$$

where we have introduced the dimensionless variables $Q = q/2k_F$, $W = \hbar\omega/4E_F$, $B = \beta/E_F$ and $M = \mu/E_F$, $\beta = 1/k_BT$, K_B is the Boltzmann's constant, and μ is the chemical potential. The quantity k_F is the Fermi wavevector, given by $k_F = (3n\pi^2)^{1/3}$, and E_F is the Fermi energy.

The chemical potential μ is obtained from the implicit expression [22]

$$B^{3/2} = \int_0^U \frac{3y}{1-y^2}\{A\ln[(1-y^2)/y^2]\}\,\mathrm{d}y \tag{5}$$

where $U = (1 + \mathrm{e}^{-A})^{-1/2}$ and $A = BM = \mu B$. For a given A, one obtains B leading to a relation between them.

The calculated resistivities of GaN:Si as a function of impurity concentration and temperature obtained using the procedure described above are presented in figure 1. The

curves present similar forms, converging to values around 1.0×10^{18} cm^{-3} for GaN:Si, which is determined to be the critical concentration N_c for the MNM transition in this system. We have used the ionization energy $E_I = 35$ meV and the electron effective mass $m_d = 0.20m_0$.

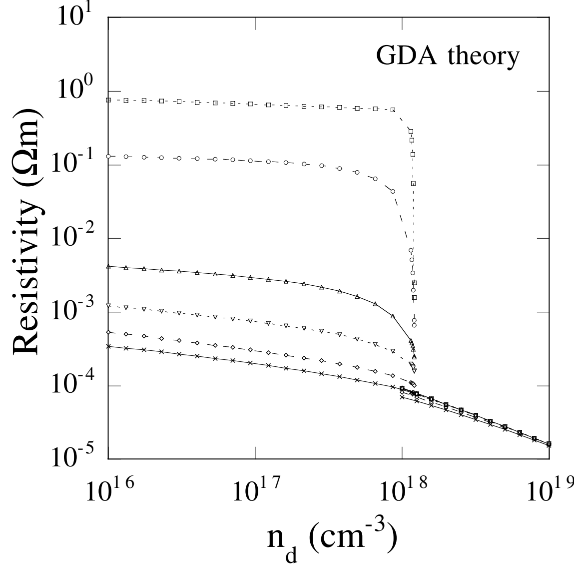

Figure 1. Resistivity of GaN:Si as a function of the donor impurity concentration n_d calculated by the generalized Drude approach (GDA) at different temperatures. The temperatures correspond, from top to bottom, to 4, 12, 50,100, 200 and 300 K.

3. BGS and discussion

The different self-energy shifts presented in the determination of the two band gap energies were calculated with many-body theory within the zero temperature formalism along the lines of [15–17, 23–25]. The signs of these self-energy shifts are such that all tend to reduce the band gap values.

GaN is a single-valley semiconductor. The Fermi volume is spherical. We characterize the band dispersion with the density-of-states effective mass. Thus we represent the Fermi volume with a sphere of radius k_F.

The single-particle energy for a state $(\boldsymbol{p}, \sigma)$ we define as the variational derivative of the total energy with respect to the occupation number for state $(\boldsymbol{p}, \sigma)$, i.e.

$$\varepsilon_{p,\sigma} = \frac{\delta(NE)}{\delta n_{p,\sigma}} = \varepsilon_p^0 + \hbar\Sigma_{p,\sigma} \tag{6}$$

where the first term on the right-hand side is the unperturbed single-particle energy (the kinetic energy) and the second is the self-energy from the interactions. With the variational derivative we mean, for $p < k_F$, minus the change in total energy when the occupation number for state $(\boldsymbol{p}, \sigma)$ is subtracted from the sum over occupied states; for $p > k_F$, we mean the change in total energy when the occupation number for state $(\boldsymbol{p}, \sigma)$ is added to the sum over occupied states. In other words we address the whole change in total energy to the energy of the single-particle state. This is the so-called Rayleigh–Schrödinger perturbation theory.

The two band gaps are obtained as

$$E_{G,1} = E_{G,0} + \varepsilon^{0,e}_{k_F} + \hbar\Sigma^{e}_{k_F,\sigma} + \hbar\Sigma^{h}_{0,\sigma}$$
$$E_{G,2} = E_{G,0} + \hbar\Sigma^{e}_{0,\sigma} + \hbar\Sigma^{h}_{0,\sigma} \tag{7}$$

where the indices e and h stand for electrons and holes, respectively .

We assume a random distribution of donors and approximate the ionized-donor potentials with pure Coulomb potentials. With these approximations the interaction energy consists of exchange, correlation, and electron–impurity, electron–electron interaction parts. The correlation energy is

$$E_c = +\mathrm{i}\int_0^1 \frac{\mathrm{d}\lambda}{\lambda}\frac{1}{2N}\sum_q{}' \left\{ \int_{-\infty}^{+\infty} \frac{\mathrm{d}\omega}{2\pi}\hbar \left[\left(\frac{1}{\varepsilon^{\lambda}(q,\omega)} - 1 \right) - \left(\frac{1}{\varepsilon^{HF,\lambda}(q,\omega)} - 1 \right) \right] \right\} \tag{8}$$

the exchange energy is

$$E_x = +\mathrm{i}\int_0^1 \frac{\mathrm{d}\lambda}{\lambda}\frac{1}{2N}\sum_q{}' \left\{ \int_{-\infty}^{+\infty} \frac{\mathrm{d}\omega}{2\pi}\hbar \left[\left(\frac{1}{\varepsilon^{HF,\lambda}(q,\omega)} - 1 \right) - \left(\frac{1}{\varepsilon_0^{\lambda}(q,\omega)} - 1 \right) \right] \right\} \tag{9}$$

the total electron–electron interaction part is

$$E_{xc} = +\mathrm{i}\int_0^1 \frac{\mathrm{d}\lambda}{\lambda}\frac{1}{2N}\sum_q{}' \left\{ \int_{-\infty}^{+\infty} \frac{\mathrm{d}\omega}{2\pi}\hbar \left[\left(\frac{1}{\varepsilon^{\lambda}(q,\omega)} - 1 \right) - \left(\frac{1}{\varepsilon_0^{\lambda}(q,\omega)} - 1 \right) \right] \right\} \tag{10}$$

and the electron–impurity interaction part is

$$E_{ion} = \frac{1}{2N}\sum_q{}' \frac{n\nu_q}{\kappa} \left(\frac{1}{\varepsilon(q,0)} - 1 \right). \tag{11}$$

Here κ is the background dielectric constant. All these energies are energies per electron. The coupling constant λ in equations (8)–(10) is the result of the so-called ground-state energy theorem. A superscript λ indicates that all Coulomb interactions are multiplied by λ. The dielectric function with the superscript HF is the dielectric function in the Hartree–Fock approximation. The approximation in equation (10) lies in the choice of dielectric function in the first term of the integrand. Choosing the Hartree–Fock dielectric function results in the exchange energy, as can be seen from equation (9). The second terms in E_x and E_{xc} represent the subtraction of the self-interaction terms and the dielectric function in these terms is an artificial function introduced to make the physics more transparent and simultaneously make the integrals converge faster. This dielectric function is the result where the electrons are distributed over the single-particle states in the usual way, obeying the Pauli principle, but are allowed to scatter into occupied states. The last energy contribution is the result to second order in the electron–impurity interaction, where ν_q is the Coulomb potential. We perform the calculation in the RPA where

$$\varepsilon(q,\omega) = 1 + \alpha_0(q,\omega) \tag{12}$$

$$\alpha_0(q,\omega) = -\frac{1}{\hbar\kappa}\nu_q \sum_\sigma{}' \int \frac{\mathrm{d}^3k}{(2\pi)^3} \int_{-\infty}^{\infty} \frac{\mathrm{d}\varepsilon}{2\pi\mathrm{i}} G_\sigma^{(0)}(k,\varepsilon) G_\sigma^{(0)}(k+q,\varepsilon+\omega) \tag{13}$$

$$G_\sigma^{(0)}(k,\varepsilon) = \frac{n_{k,\sigma}}{\varepsilon - (\hbar k^2/2m^*) - \mathrm{i}\eta} + \frac{1 - n_{k,\sigma}}{\varepsilon - (\hbar k^2/2m^*) - \mathrm{i}\eta} \tag{14}$$

$$n_{k,\sigma} = \begin{cases} 1 & \text{if } k < k_F \\ 0 & \text{otherwise.} \end{cases} \tag{15}$$

From these relations we see how the occupation numbers enter the energy expressions. To get the self-energy shift for the valence-band holes we add a small fraction of holes; these

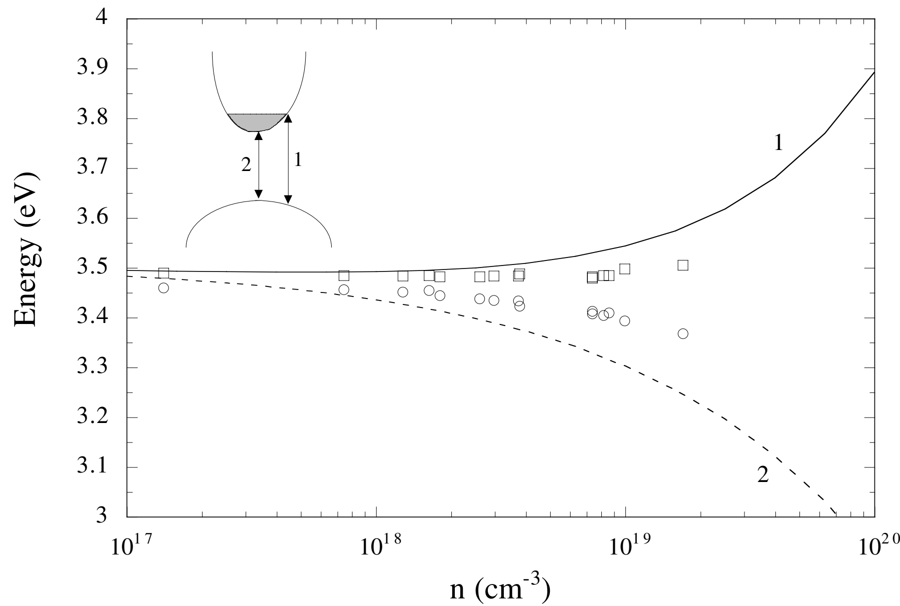

Figure 2. Calculated (RPA approximation) and experimental band gap energies for GaN:Si as a function of ionized impurity concentration. The full curve represents the transition 1 between the Fermi level E_F and the state at the valence band, VB. It corresponds to the optical band gap $E_{G,1}$. The dotted curve represents the transition 2 between the bottom of the conduction band, CB, and the extremum of the VB. It corresponds to the reduced band gap, $E_{G,2}$. The open squares and circles are the experimental data [14], which correspond to $E_{G,1}$ and $E_{G,2}$ respectively. The parameters used are $E_{G,0} = 3.52$ eV, $\varepsilon = 9.5$, $m_d = 0.20m_0$, $m_{hh} = 0.55m_0$ and $m_{lh} = 0.55m_0$.

holes give rise to an additional polarizability term in the dielectric function. This term can be expressed in terms of Green's functions for the holes in analogy with the above expression and in that way the occupation numbers for the hole states enter the energy expressions. When the functional derivatives with respect to hole occupation numbers have been taken the hole polarizabilities are allowed to go to zero. For more details of the calculation see [15, 17–25]. In figures 2 and 3 we show the results for different transitions in comparison to the experimental data [14], represented by empty squares and circles, which are expected to be the optical, $E_{G,1}$, and reduced, $E_{G,2}$, band gap energies, respectively. A reasonable agreement is found between experiment and theory for these transitions. These two figures represent two different approximations. In the real system the valence band consists of two bands; one heavy-hole band; one light-hole band. These bands are degenerate in the Γ-point. The bands are coupled and holes can scatter from one band to the other. This coupling has the effect that the states at the Γ-point are shifted the same amount when the system is doped. Our code does not include this coupling for hexagonal systems. In one situation, when the masses of the two bands are equal, the coupling has no effect at all. To get a feeling for how serious this deficiency in the code is we have made one calculation using the same masses, figure 2, and one using different masses, figure 3. In figure 2, the valence-band degeneracy is lifted. If the coupling had been included the degeneracy would have prevailed and the shift of the valence bands at the Γ-point would have been the same as in figure 2.

We now perform the calculation of BGS using Lindefelt's model [19], which is an extension of the approach originally developed by Jain *et al* [18]. The latter is partly based on the

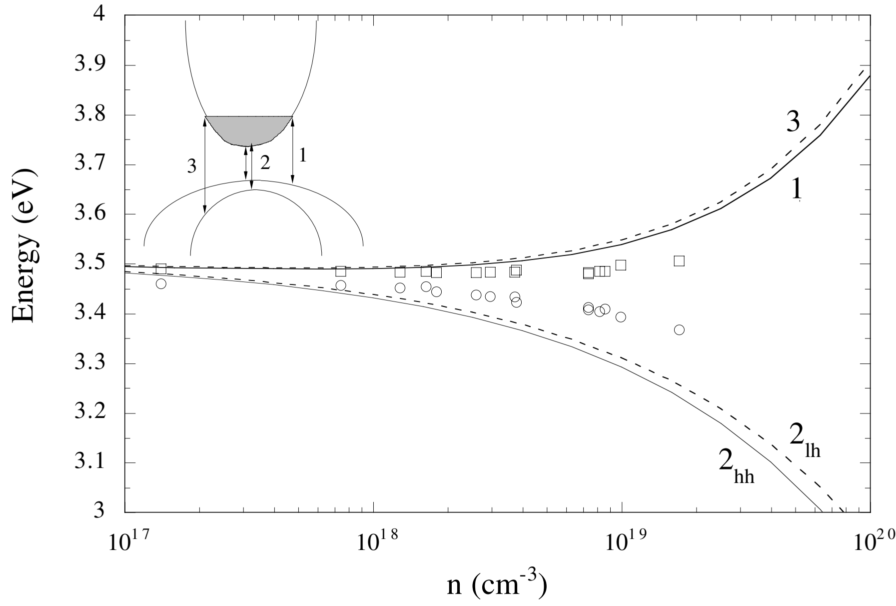

Figure 3. Calculated (RPA approximation) and experimental band gap energies for GaN:Si as a function of ionized impurity concentration. The upper full curve represents the transition 1 between E_F and the uppermost VB, which is the heavy-hole (hh) band. The upper dashed curve represents the transition 3 between E_F and the lower VB, which is the light-hole (lh) band. Both cases correspond to $E_{G,1}$. The lower full curve represents the transition 2, between the bottom of the CB and the hh band. The lower dashed curve represents the transition 2 between the bottom of the CB and the lh band. Both cases correspond to $E_{G,2}$. The open squares and circles are the experimental data [14], which correspond to $E_{G,1}$ and $E_{G,2}$, respectively. The parameters used are $E_{G,0} = 3.52$ eV, $\varepsilon = 9.5$, $m_d = 0.20m_0$, $m_{hh} = 0.60m_0$ and $m_{lh} = 0.51m_0$.

plasmon-pole approximation and partly on the RPA [17]. Even though the model in Lindefelt uses several approximations as a constant dielectric function, parabolic energy bands, and a parabolic approximation of the overlap integrals for cubic materials, with emphasis on the hole–donor interaction, it fairly accurately describes both the lowest conduction band and the uppermost valence band, which are not described in Jain *et al* [18]. Lindefelt's model is described as follows.

The reduced band gap is written as [16]

$$E_{G,2} = E_{G,0} - \Delta E_G \tag{16}$$

where $E_{G,0}$ is the band gap energy for undoped material and ΔE_G is the BGS. The corresponding optical band gap is

$$E_{G,1} = E_{G,2} - \Delta E_G^{BM} \tag{17}$$

where ΔE_G^{BM} is the Burstein–Moss shift [26, 27]. It is written as and

$$\Delta E_G^{BM} = \frac{\hbar^2 k_F^2}{2m_d}\left(1 + \frac{m_d}{m_h}\right). \tag{18}$$

In equations (17) and (18), m_d and m_h are the density-of-states effective masses of the majority and minority carriers, respectively. The shift of the band gap due to doping has contributions from both the shift of the conduction band, ΔE_c, and the shift of the valence band, ΔE_v, and it is written as

$$\Delta E_G = -\Delta E_c + \Delta E_v. \tag{19}$$

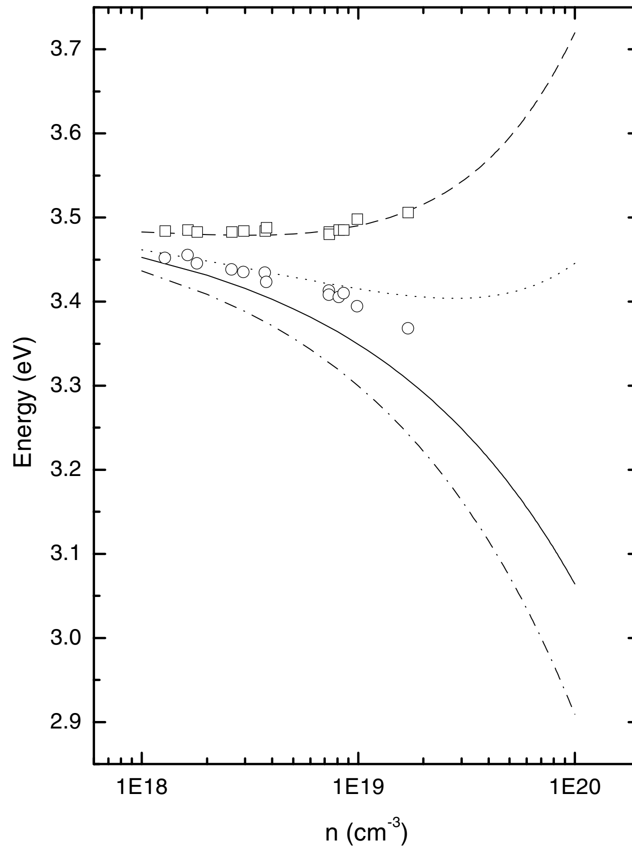

Figure 4. Calculated (two different models) and experimental band gap energies for GaN:Si as a function of ionized impurity concentration. The dashed and the full curves represent $E_{G,1}$ and $E_{G,2}$, respectively, from the Jain *et al* model [18]. The dotted and dot-dashed curves represent $E_{G,1}$ and $E_{G,2}$, respectively, from the Lindefelt model [19]. The open squares and circles are the experimental data [14]. The parameters used are the same as for figure 2.

ΔE_c is a positive quantity and ΔE_v is a negative quantity, implying that both contributions reduce the band gap as follows [19]:

$$\Delta E_c = \hbar \sum_c^{ee} + \hbar \sum_c^{ed} \tag{20}$$

$$\Delta E_v = \hbar \sum_v^{he} + \hbar \sum_v^{hd}. \tag{21}$$

In equation (20) the first term on the right-hand side is the self-energy for electron–electron interactions of the conduction band electron gas and the second term is the self-energy of the interaction between the conduction band electron and the donors ions. In equation (21) the first term on the right-hand side is the self-energy of a hole in the valence band as it moves through the electron gas of the conduction band electrons and the second term is the self-energy for interaction holes with the donors ions. They are written as

$$\hbar \sum_c^{ee} = -13.6 \times 3\left(\frac{a_0}{\varepsilon}\right)\left(\frac{3}{\pi}n\right)^{1/3} \tag{22}$$

$$\hbar \sum_{c}^{ed} = -13.6\left(\frac{\pi^3}{3}\frac{a_0^3}{\varepsilon m_d}\right)^{1/2} n \tag{23}$$

$$\hbar \sum_{v}^{hd} = 13.6\left(\frac{\pi^3}{3}\right)^{1/2} \frac{m_{hh}^* + m_{lh}^*}{2\varepsilon^{1/2}} \left(\frac{a_0}{m_d}\right)^{3/2} n^{1/2} \tag{24}$$

$$\hbar \sum_{v}^{he} = 13.6\left(\frac{4}{\pi^{3/4}}\right)\left(\frac{m_d a_0^3}{\varepsilon^5}\right) J^{(e)} n^{1/4}. \tag{25}$$

In the equations above, a_0 is the Bohr radius, k is the dielectric constant of the material, m_{lh} is the light-hole effective mass, and m_{hh} is the heavy-hole effective mass. The integral $J^{(e)}$ is defined as [19],

$$J^{(e)} = \frac{1}{2}\sum_{v=lh}^{hh} J_v(S_0^e) \qquad S_0^e = \frac{\hbar\omega_p}{E_F} \tag{26a}$$

$$J_v(S_0^{(e)}) = \int_0^\infty \frac{\mathrm{d}S}{\Omega^{(e)}(s)} \frac{1}{\Omega^{(e)}(s) + (m_d/m_v)S^2} \tag{26b}$$

$$\Omega^{(e)}(S) = \sqrt{1 + \frac{4}{3}\frac{S}{S_0^{(e)}} + S^2}. \tag{26c}$$

In equation (26*a*) E_F is the Fermi energy and ω_p is the plasma frequency of the electron.

We have considered $E_{G,0} = 3.52$ eV, the dielectric constant $\varepsilon = 9.5$, $m_{hh} = 0.55m_0$, $m_{lh} = 0.55m_0$, and $m_d = 0.20$.

In figure 4 we show the results of the Lindefelt and Jain *et al* models.

4. Summary

We have investigated the electrical resistivity, the MNM transition, and the possible optical transition involved in the experimental measurements for Si-doped wurtzite GaN which lead to the BGS. The variation of the BGS appears for values above the critical concentration for the MNM transition, which is estimated when all the resistivity curves merge together to one critical point. The calculations for the BGS were carried out within a framework of the RPA. In the light of a very recent photoluminescence measurement, we have investigated and discussed all the possible transitions involved with a reasonable agreement with them. It is worth pointing out that a full band structure calculation with all possible transition energies including a very accurate Burstein–Moss shift is required to explain the experimental results more precisely.

Acknowledgments

This work was sponsored by the Brazilian funding agencies CNPq and CAPES, US Department of Energy under contract No DE-AC05-00OR22725 with Oak Ridge National Laboratory, managed by UT-Battelle, Limited Liability Corporation (LLC) and Swedish Research Council for Engineering Sciences (TFR). The authors acknowledge a very fruitful correspondence with Joachim Wagner.

References

[1] Morkoç H, Strite S, Gao G B, Lin M E, Sverdlov B and Burns M 1994 *J. Appl. Phys.* **76** 1363
[2] Nakamura S 1999 *Semicond. Sci. Technol.* **14** R27

[3] Li Z Q *et al* 2000 *Appl. Phys. Lett.* **76** 3765
[4] Chen G D, Smith M, Lin J Y, Jiang X X, Wei S-H, Asif Khan M and Sun C J 1996 *Appl. Phys. Lett.* **68** 2784
[5] Monemar B 1999 *J. Mater. Sci.* **10** 227
[6] Jain S C, Willander M, Narayan J and Van Overstraeten R 2000 *J. Appl. Phys.* **87** 965
[7] Lima A P, Tabata A, Leite J R, Kaiser S, Schikora D, Schöttker B, Frey T, As D J and Lischka K 1999 *J. Crystal Growth* **201/202** 396
[8] Fernandez J R L, Chitta V A, Abramof E, Ferreira da Silva A, Leite J R, Tabata A, As D J, Frey T, Schikora D and Lischka K 2000 *MRS Internet J. Nitride Semicond. Res.* **5** (Suppl. 1) U191–U196
[9] Stampfl C and Van de Walle C G 1999 *Phys. Rev.* B **59** 5521
[10] Kawashima T, Yoshikawa H, Adachi S, Fuke S and Ohtsuka K 1997 *J. Appl. Phys.* **82** 3528
[11] Lee I H, Lee J J, Kung P, Sanchez F J and Razeghi M 1999 *Appl. Phys. Lett.* **74** 102
[12] Neugebauer J and Van de Walle C G 1996 *Appl. Phys. Lett.* **69** 503
[13] Schubert E F, Goepfert I D, Grieshaber W and Redwing J M 1997 *Appl. Phys. Lett.* **71** 921
[14] Yoshikawa M, Kunzer M, Wagner J, Obloh H, Schlotter P, Schmidt R, Herres N and Kaufmann U 1999 *J. Appl. Phys.* **86** 4400
[15] Moysés Araújo C, Souza de Almeida J, Pepe I, Ferreira da Silva A, Sernelius Bo E, Pereira de Souza J and Boudinov H 2000 *Phys. Rev.* B **62** 12 882
[16] Ferreira da Silva A, Persson C, Marcussen M C B, Veje E and de Oliveira A G 1999 *Phys. Rev.* B **60** 2463
[17] Berggren K-F and Sernelius Bo E 1981 *Phys. Rev.* B **24** 1971
[18] Jain S C, McGregor J M and Roulston D J 1990 *J. Appl. Phys.* **68** 3747
[19] Lindefelt U 1998 *J. Appl. Phys.* **84** 2628
[20] Sernelius Bo E and Morling M 1988 *Proc. 3rd Int. Conf. on Shallow Impurities in Semiconductors (10–12 August 1988, Linköping, Sweden)*
[21] Sernelius Bo E 1987 *Phys. Rev.* B **36** 1080
[22] Ferreira da Silva A, Sernelius Bo E, de Souza J P, Boudinov H, Zheng H and Sarachik M P 1999 *Phys. Rev.* B **60** 15 824
[23] Rice T M 1965 *Ann. Phys.* **31** 100
[24] Sernelius Bo E 1986 *Phys. Rev.* B **34** 5610
[25] Persson C, Lindefelt U and Sernelius Bo E 1999 *Phys. Rev.* B **60** 16 479
[26] Burstein E 1954 *Phys. Rev.* **93** 632
[27] Moss T M 1954 *Proc. Phys. Soc. London* B **67** 775